

Fig. 1. Overexpression of wild-type APP but not a mutant APP that is unable to produce A β reduces excitatory postsynaptic current (EPSC) size without altering the paired-pulse ratio (PPR); overexpression of APP also reduces mEPSC amplitude and frequency. (A) Immunoprecipitation by using 6E10 of [35 S]methionine-labeled APP (Upper) and A β (Lower) from cells and medium showed that infection with viral constructs encoding either APP or APP Δ BACE directed expression of full-length, cell-associated APP and secreted APP α in medium. Viral constructs encoding GFP served as a control for these experiments. Only neurons overexpressing wild-type APP generated significant levels of A β . (B) Average EPSC size was reduced in neurons overexpressing wild-type APP (0.62 of GFP-alone control; *, $P < 0.05$) but not in neurons overexpressing APP Δ BACE. Traces show typical paired-pulse responses from each group with action currents blanked for clarity. (Scale bar, 1.5 nA, 10 ms.) (C) There was no difference in the PPR, measured as the relative sizes of the first and second responses to a pair of stimuli delivered 50 ms apart, in neurons overexpressing wild-type APP or APP Δ BACE compared with GFP-alone-expressing neurons. (D) There was a small but significant decrease in mEPSC size (0.85 of control; *, $P < 0.02$) and a reduction in mEPSC frequency (0.56 of control; *, $P < 0.04$) in neurons overexpressing wild-type APP. For these mEPSC experiments, results from uninfected and GFP-expressing neurons, which were indistinguishable, were combined for the control group. Traces show typical spontaneous responses from control and APP-overexpressing neurons. (Scale bar, 20 pA, 100 ms.)

(IRES) cassette downstream from the APP sequence. Fig. 1A shows that cultured neurons overexpressing either wild-type APP or APP Δ BACE produced cell-associated full-length APP. Both wild-type and mutant APP underwent α -secretase-mediated cleavage and secretion of APP α into the medium, detected by immunoprecipitations with 6E10 antibody. As expected, however, only wild-type APP generated significant levels of A β . Thus, neurons expressing APP Δ BACE provided a control for the effects of viral-mediated APP overexpression and post-translational processing by the nonamyloidogenic α -secretase pathway. Neurons expressing only GFP served as additional non-APP controls.

APP Overexpression Silences Synapses, Likely Through an A β -Mediated Mechanism. To study the acute effects of APP overexpression on synaptic transmission, we performed whole-cell voltage clamp recordings on isolated autaptic neurons at 10–17 days in culture. Fig. 1B shows that EPSC amplitudes were significantly reduced in neurons overexpressing wild-type APP, relative to GFP controls (GFP, 3,535 \pm 430 pA, $n = 26$; APP, 2,228 \pm 286 pA, $n = 25$; $P < 0.05$). In contrast, expression of mutant APP Δ BACE had no significant effect on EPSC size (APP Δ BACE, 3,230 \pm 347 pA, $n = 28$), indicating that A β was responsible for the decrease in EPSC size in cells overexpressing wild-type APP.

A decrease in evoked-response amplitude could result from negative modulation of the presynaptic release machinery. Thus, we monitored the PPR, a measure that is inversely related to presynaptic release probability (22). Fig. 1C shows that APP overexpression did not alter the PPR relative to GFP controls (GFP, 0.82 \pm 0.03, $n = 26$; APP, 0.83 \pm 0.04, $n = 25$). Similarly, overexpression of APP Δ BACE did not alter PPR relative to control neurons (APP Δ BACE, 0.81 \pm 0.03, $n = 28$). The lack of change in the PPR for neurons overexpressing APP strongly suggests that there was no change in synaptic release probability at individual presynaptic sites.

We also assessed the effect of APP overexpression on spontaneous miniature EPSCs (mEPSCs). The small but significant decrease in mEPSC amplitude relative to uninfected and GFP-alone controls [Fig. 1D and supporting information (SI) Fig. 5; control, 26.5 \pm 1.03 pA, $n = 25$; APP, 22.6 \pm 1.24 pA, $n = 25$; $P < 0.02$] suggests that a reduction in the number (or function) of postsynaptic AMPARs at individual synapses contributes to the decrease in EPSC size, although a presynaptic reduction in the amount of transmitter packaged per vesicle (reduced quantal size) could also account for reduced mEPSC size. Note, however, that the discrepancy between the magnitude of reduction in EPSC and mEPSC amplitudes means that additional mechanisms must account for the greater reduction in EPSC size. The large decrease in mEPSC frequency (control, 4.3 \pm 0.7 Hz, $n = 25$; APP, 2.4 \pm 0.4, $n = 20$; $P < 0.04$) suggests that these additional mechanisms might include a presynaptic silencing of release sites and/or a postsynaptic silencing produced by complete removal of AMPARs at individual synapses.

APP Overexpression Selectively Reduces AMPAR-Mediated Transmission. To test directly the possibility that modification of the number (or function) of postsynaptic glutamate receptors contributes to APP-mediated synaptic silencing, the relative amplitudes of the AMPAR-mediated and NMDA receptor-mediated (NMDAR-mediated) components of synaptic responses were measured in neurons overexpressing APP. Fig. 2 shows the selective reduction in the AMPAR-mediated component of the EPSC in neurons overexpressing APP compared with APP Δ BACE, and uninfected and GFP-alone combined controls (control, 6,203 \pm 417 pA, $n = 31$; APP Δ BACE, 5,216 \pm 845 pA, $n = 11$; APP, 3,953 \pm 523 pA, $n = 22$; $P < 0.01$), with no change in the NMDAR-mediated component (control, 1,966 \pm 139 pA, $n = 31$; APP Δ BACE, 1,921 \pm 346 pA, $n = 11$; APP, 1,775 \pm 260

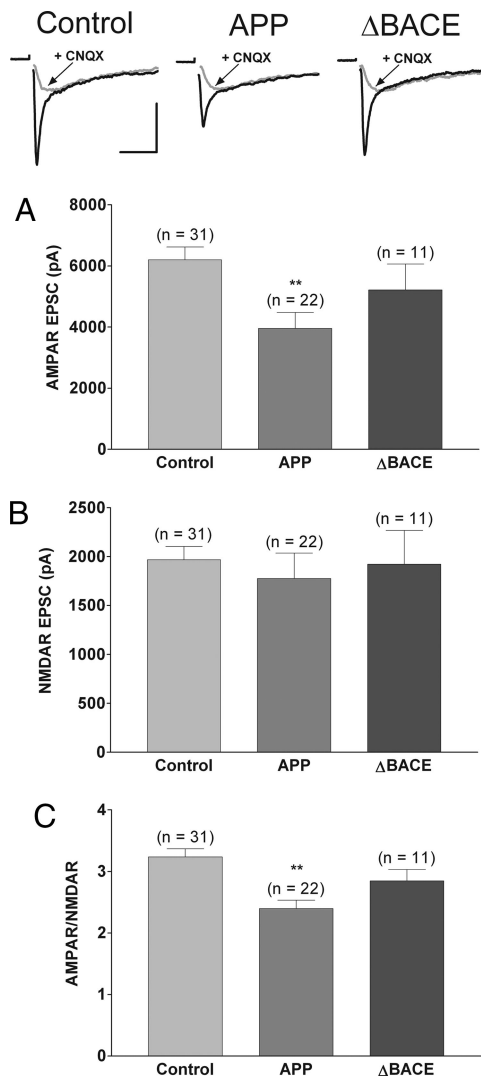


Fig. 2. Overexpression of APP but not APP_{ΔBACE} reduces the AMPAR/NMDAR amplitude ratio by selectively decreasing AMPAR-mediated currents. (Top) Representative EPSCs recorded in Mg²⁺-free external solution ± 10 μM 6-cyano-7-nitroquinoline-2,3-dione (CNQX) with action currents blanked for clarity. (Scale bars, 3 nA, 20 ms.) (A) Summary of average AMPAR-mediated EPSC peak amplitude showing a significant reduction in neurons overexpressing APP (0.64 of control; **, $P < 0.01$). (B) Summary of average NMDAR-mediated EPSC peak amplitude showing no change in neurons overexpressing APP. (C) Summary of average AMPAR/NMDAR amplitude ratios for control neurons and neurons overexpressing APP (0.74 of control; **, $P < 0.01$). For these experiments, uninfected and GFP-expressing neurons, which were indistinguishable, were combined for the control group.

pA, $n = 22$). This selective reduction led to a significant decrease in the ratio of currents mediated by AMPARs vs. NMDARs (AMPAR/NMDAR ratio; control, 3.2 ± 0.1 , $n = 31$; APP_{ΔBACE}, 2.9 ± 0.2 , $n = 11$; APP, 2.4 ± 0.1 , $n = 22$; $P < 0.01$). Together with the decrease in the AMPAR-dominated mEPSC amplitude, these data point to a postsynaptic mechanism underlying the reduction in EPSC size, and they argue strongly against changes in the amount of transmitter packaged per vesicle as a mechanism to account for decreased EPSC size, given the lack of change in NMDAR-mediated currents.

APP Overexpression Does Not Silence Sites Presynaptically. Although the lack of change in NMDAR-mediated currents in neurons overexpressing APP argues against a presynaptic silencing of

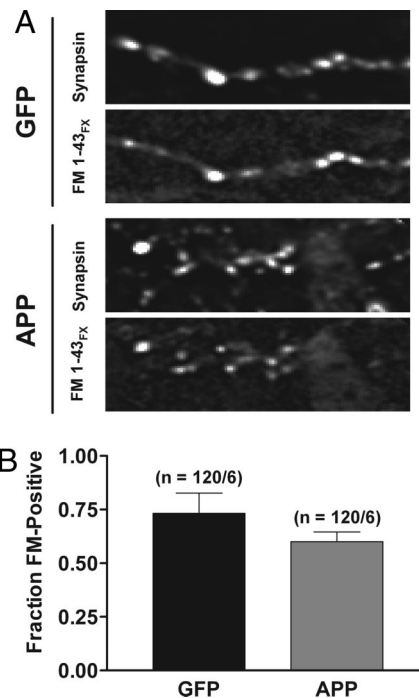


Fig. 3. APP overexpression does not alter the fraction of presynaptically active synapses. (A) Raw fluorescent images show puncta labeled with anti-synapsin antibody and fixable FM1-43_{FX} in synapses expressing GFP alone (Upper) and in synapses overexpressing APP (Lower). (B) The fraction of synapsin-positive puncta that colabeled with FM1-43_{FX} was not significantly different in neurons overexpressing APP.

release sites, we tested this possibility directly by monitoring the fraction of puncta labeled by antibodies against the presynaptic vesicle protein synapsin that were colabeled with the fixable form of the dye FM1-43 (FM1-43_{FX}). The colabeled fraction reports functional release sites that undergo active vesicle recycling. In cells overexpressing APP, there was no significant change in the number of synapsin-positive sites that were colabeled with FM1-43_{FX} compared with GFP controls (Fig. 3; GFP, 0.73 ± 0.09 , $n = 120$ puncta from 6 fields; APP, 0.63 ± 0.05 , $n = 120$ puncta from 6 fields). These data show that presynaptic silencing does not contribute to APP-mediated synaptic depression.

APP Overexpression Alters the Kinetics of Synaptic Vesicle Cycling but Not the Rate of Refilling of the Readily Releasable Pool (RRP), nor the Size of the Cycling Pool. Although we found no evidence for a change in release probability at individual presynaptic sites, APP overexpression could still act presynaptically to alter the rate at which the RRP is refilled from the reserve pool, the rate at which the reserve pool is refilled with recycling vesicles, and/or the size of the total cycling pool of vesicles, any of which could affect sustained release during long trains of action potentials. To test for changes in the rate at which the RRP is refilled from the reserve pool, cells were stimulated at 20 Hz for 1.5 s to deplete the RRP (23), after which refilling was probed by monitoring the extent to which the EPSC recovered at 1.5 s after the end of the train. There was no difference in the extent of recovery in neurons overexpressing APP (Fig. 4A; GFP, 0.79 ± 0.03 of initial value, $n = 48$; APP, 0.79 ± 0.03 , $n = 49$), showing that there was no change in the rate at which the RRP was refilled. Note also that the identical rate of depression during depletion of the RRP with 20 Hz stimulation suggests that the size of the RRP at individual release sites is unchanged by APP overexpression (24).

To probe for changes in vesicle cycling that might not be apparent with single stimuli or brief trains, we loaded synapses

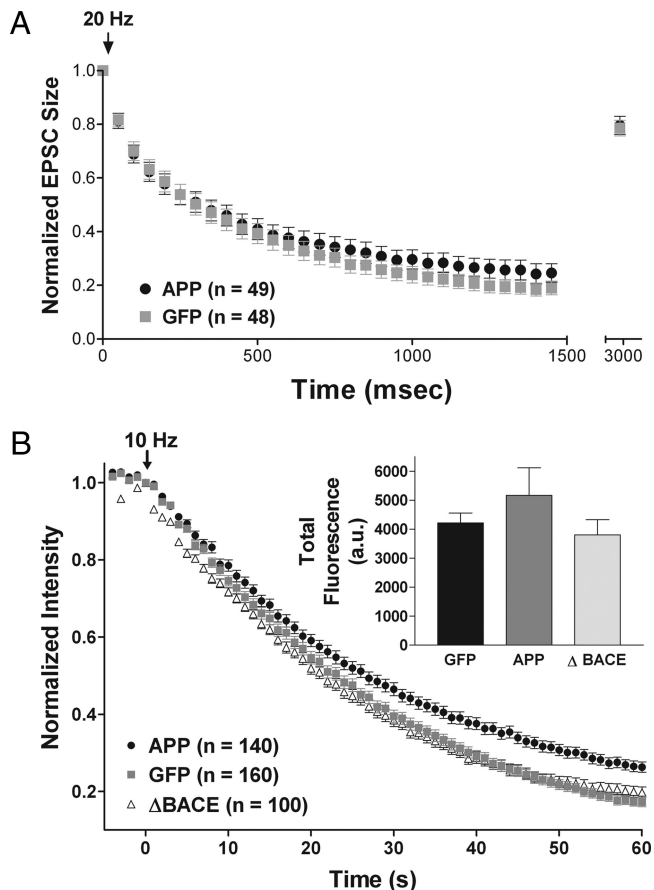


Fig. 4. Overexpression of APP has no effect on depression during a brief train, refilling of the RRP, or size of the cycling vesicle pool, but it reduces the rate of FM destaining, likely through an $A\beta$ -mediated mechanism. (A) EPSC amplitudes in response to a 20-Hz train of stimuli lasting 1.5 s depressed at comparable rates in APP- and GFP-alone-expressing neurons. The amplitude of a single EPSC evoked 1.5 s after the end of the train was used to measure recovery from depletion of the pool of readily releasable vesicles. Each data point was normalized to the initial EPSC amplitude. (B) Time course of FM 4-64 fluorescence changes of puncta in neurons expressing APP, APP Δ BACE, or GFP alone during electrical field stimulation at 10 Hz (arrow marks start of stimulation at time 0), plotted as mean fluorescence of each individual puncta normalized to the value immediately preceding stimulation. (Inset) Average total releasable fluorescence of individual sites; there was no difference among groups.

with red fluorescent FM4-64 dye, and we performed optical imaging experiments monitoring the rate of dye loss during 60-s trains of stimulation delivered at 10 Hz (Fig. 4B). Neurons overexpressing APP lost FM fluorescence from dye-loaded synapses more slowly than GFP controls (GFP, $t_{1/2} = 25.8 \pm 1.9$ s, $n = 160$ puncta from 8 fields; APP, $t_{1/2} = 31.8 \pm 1.6$ s, $n = 140$ puncta from 7 fields; $P < 0.05$). This effect was not seen with overexpression of the APP Δ BACE mutant (APP Δ BACE, $t_{1/2} = 25.6 \pm 1.2$ s, $n = 100$ puncta from 5 fields), suggesting that $A\beta$ is responsible for the decrease in destaining rate, which may reflect a deficit in the rate at which recycled vesicles replenish the reserve pool. The total amount of releasable fluorescence loaded did not change with APP overexpression (GFP, $4,216 \pm 344$ a.u.; APP, $5,171 \pm 949$ a.u.; APP Δ BACE, $3,805 \pm 528$ a.u.), indicating that there was no change in the size of the total cycling pool of synaptic vesicles.

Discussion

With our current study, we rule out a presynaptic contribution to the APP-mediated synaptic silencing observed in our sys-

tem, and we identify postsynaptic changes in AMPARs as the primary mechanism responsible for depression of responses evoked by single action potentials or brief trains. With very long trains of action potentials, we could also identify a presynaptic deficit in vesicle cycling in neurons overexpressing APP. These pre- and postsynaptic effects are most likely mediated by $A\beta$, although a role for two other BACE-dependent APP cleavage products, β -C-terminal fragment and secreted APPs β , cannot be ruled out.

Although the small decrease in mEPSC amplitude shows that AMPAR-mediated currents are reduced at some synapses that remain responsive to transmitter release, the large decrease in mEPSC frequency as well as the discrepancy between the magnitude of the effect on EPSC and mEPSC amplitudes suggest that AMPAR-mediated currents are lost entirely at a sizable fraction of synapses affected by APP overexpression. Because NMDAR-mediated currents are unaltered, the fraction of classically defined "silent synapses," i.e., those that contain only NMDAR-mediated responses without any AMPAR-mediated component, must rise with APP overexpression. The simplest explanation is that AMPARs are trafficked away from postsynaptic sites, but other mechanisms (e.g., changes in affinity for glutamate or other channel properties) could also explain this postsynaptic silencing.

A postsynaptic silencing caused by selective removal of AMPARs is consistent with Chang *et al.* (19), who found a decrease in AMPAR-mediated currents but not NMDAR-mediated currents in aged 2XKI AD model mice; this effect could be attributed to a reduction in the number of postsynaptic AMPARs evaluated by EM immunocytochemistry. This hypothesis is also supported by findings that application of $A\beta$ reduces mEPSC amplitude in cortical slices (17), and it reduces surface levels of GluR1 and GluR2 AMPA receptor subunits in cultured cortical neurons (15, 16). Curiously, Chang *et al.* (19) did not observe a decline in the frequency of mEPSCs. A possible explanation for this discrepancy is that their study monitored effects at a time point "earlier" in the disease state than our model system, that is, at a point when receptors have been reduced but not entirely eliminated from individual synapses.

Our results also differ from Kamenetz *et al.* (14), who found a significant reduction in both AMPAR- and NMDAR-mediated currents. Very recent work from the Malinow group indicates that $A\beta$ -mediated removal of AMPARs triggers the retraction of dendritic spines, consequently removing NMDARs from the synapse (R. Malinow, personal communication; see also ref. 25). Thus, by recording at times slightly longer after viral infection than in our study, Kamenetz *et al.* (14) may have observed effects that occur at a later stage of $A\beta$ -induced synaptic dysfunction. It is of interest that neurons lacking APP show enhanced AMPAR- and NMDAR-mediated currents as well as elevated mEPSC frequencies, all of which can be explained by an increase in the number of immunologically detected synapses (26), supporting the proposal by Kamenetz *et al.* (14) that modulation of synapses by APP is a normal process that becomes pathologically hyperactive at the onset of AD.

In addition to identifying a postsynaptic deficit that could account for the APP-mediated effects on EPSC size and mEPSC frequency, we also observed a presynaptic deficit in vesicle cycling during extended trains of stimulation, monitored by FM destaining. The lack of effect of APP up-regulation on basal release probability or refilling of the RRP from the reserve pool of vesicles implicates an impairment of the process by which exocytosed vesicles are retrieved and returned to the reserve pool. This possibility could be explained by a reduction in dynamin 1, the GTPase responsible for pinching off synaptic vesicles during their endocytic retrieval from the plasma membrane; indeed, levels of dynamin 1 are significantly reduced in

AD brains (20), and A β application significantly decreases dynamin 1 levels in cultured hippocampal neurons (27). Deficits in vesicle retrieval would not be expected to influence responses evoked by single action potentials or brief trains, but they could lead to suppression of transmission during sustained bursts of action potentials, and in this way they may disrupt neural circuits involved in cognition.

In summary, we find that overexpression of APP depresses transmission through both presynaptic and postsynaptic mechanisms, with selective removal of AMPARs accounting for the majority of observed effects.

Methods

Neuronal Cultures. Neurons isolated from the hippocampi of P0–P1 wild-type mice were cultured on small microislands of permissive substrate as described in ref. 28. Neurons were plated onto a feeder layer of astrocytes laid down 1–7 days earlier, then they were grown without mitotic inhibitors and used for recordings after 10–17 days in culture.

Viral Constructs. Hippocampal neurons were infected with SFV virions encoding human APP₆₉₅ (wild-type or mutant) and fluorescent GFP as a real-time visual reporter of infection. To make the APP_{ΔBACE} mutant, we used the QuikChange PCR strategy (Stratagene, La Jolla, CA) to introduce the M596V amino acid substitution (21) into a wild-type APP construct in pIRES2-GFP (Clontech, Mountain View, CA). The coding regions of all constructs were confirmed by sequencing. The wild-type or mutant APP-IRES-GFP coding regions were then subcloned into the pSFV vector (Invitrogen, Carlsbad, CA; ref. 29). Virions were generated according to the SFV Expression System manual. Expression of all constructs was verified by immunocytochemistry using Zymed rabbit polyclonal anti-APP (Invitrogen). All experiments are performed in accordance with University of Washington Environmental Health and Safety approved protocols.

Electrophysiology. Ten to 24 h after infection, whole-cell voltage clamp recordings were made from excitatory neurons with large spherical cell bodies by using an Axopatch 200A or MultiClamp 700A amplifier (Axon Instruments, Sunnyvale, CA). The standard extracellular solution contained 119 mM NaCl, 5 mM KCl, 2.5 mM CaCl₂, 1.5 mM MgCl₂, 30 mM glucose, 20 mM Hepes, and 1 μ M glycine. For measuring AMPAR- and NMDAR-mediated responses, Mg²⁺ was removed from the external solution (to relieve blockade of NMDARs at hyperpolarized holding potentials). After collection of control traces, 10 μ M CNQX [or 6,7-dinitroquinoxaline-2,3-dione (DNQX); Tocris (Ellisville, MO) or Ascent Scientific (Weston-Super-Mare, U.K.)] was puffed over the entire island by using a Picospritzer III (Parker Instrumentation, Fairfield, NJ) to block completely the AMPAR-mediated currents; the remaining current was mediated by NMDARs, and the AMPAR component was obtained by mathematical subtraction of the recorded traces. Recording pipettes of 2–5 M Ω were filled with 148.5 mM potassium gluconate/9 mM NaCl/1 mM MgCl₂/10 mM Hepes/0.2 mM EGTA; the chloride concentration in this solution facilitates the distinction between excitatory (glutamatergic) and inhibitory (GABAergic) autapses. Access resistance was monitored, and only cells with stable access resistance were included in the data analysis. The membrane potential was held at –60 mV, and trains of up to 30 synaptic responses were evoked every 20–40 s by triggering unclamped “action currents” with a series of 0.5-ms depolarizing steps to 40 mV delivered at 10–20 Hz. The size of the recorded responses was calculated as peak amplitude. Spontaneous mEPSCs were recorded continuously over 10-s periods. Peak amplitudes of spontaneous mEPSCs were measured

offline semiautomatically by using an adjustable amplitude threshold. All deflections from baseline greater than threshold were detected. Selected events were then visually examined, and any spurious events were manually rejected, and any missed events were flagged for inclusion in the mean amplitude and frequency calculations. mEPSC frequencies were calculated by dividing the total number of mEPSC events by the total time sampled.

FM Dye Loading, Destaining, Imaging, and Analysis. The relative probability of release and the size of the readily releasable pool were measured optically by labeling all of the vesicles in the readily releasable pool with FM4-64 (red variant), to allow proper visualization in GFP-expressing cells. FM4-64 (10 μ M; sold as SynaptoRed C2; Biotium, Hayward, CA) was bath-applied while eliciting a train of 600 action potentials at a rate of 10 Hz (to load the total cycling pool) by using field electrodes delivering 50 V/cm pulses. Ten micromolar CNQX (or DNQX; both from Tocris or Ascent Scientific) and 50 mM D-2-amino-5-phosphonovalerate (D-APV) (Tocris or Ascent Scientific) were included to prevent recurrent excitation. The FM solution was left on the cells for 60 s before perfusion with dye-free solution for 10 min. Optical imaging was done with a MicroMAX CCD camera (Princeton Instruments, Monmouth Junction, NJ). Images were acquired by computer by using WinView software (Princeton Instruments) and analyzed with ImageJ (National Institutes of Health, Bethesda, MD). Fluorescence was calculated in intensity units integrated over the pixels corresponding to a single synapse. Background fluorescence value was obtained at the end of the destaining stimulus protocol (3 \times 600 action potentials elicited at 10 Hz, with a 1-min rest between bouts of stimulation), and it was subtracted from all frames to give total releasable fluorescence. FM1-43_{FX}, the fixable variant of FM (AM1-43; Biotium), was used to label active synapses with high (60 mM) potassium solution applied for 1 min. After a 5-min wash with dye- and calcium-free solution, 300 μ M ADVASEP (CyDex, Lenexa, KS) was applied for 2 min, followed by 500 μ M SCAS (Biotium) for 5 min, to quench residual surface labeling. Fixation of dye was achieved with paraformaldehyde fixation (see below). Images for colabeling experiments were acquired on a DeltaVision microscope (Applied Precision, Issaquah, WA) at the W. M. Keck Center for Advanced Studies in Neural Signaling (University of Washington School of Medicine).

Immunocytochemistry. Cultured hippocampal neurons were fixed by bathing in 4% paraformaldehyde plus 4% sucrose in PBS for 20 min at room temperature, and then they were permeabilized by 0.2% Triton X-100 in PBS for 10 min at 4°C (or 0.01% Triton X-100 for 15 min for FM1-43_{FX} experiments to minimize loss of dye). Cells were pretreated for 30 min with blocking solution (5% BSA in PBS) at 4°C, and then they were incubated with anti-APP (rabbit polyclonal; Invitrogen), or antisynapsin (rabbit polyclonal, Chemicon, Temecula, CA) as a general presynaptic marker, at 1:1000 dilution in blocking solution for 1 h at room temperature. Neurons were incubated with an appropriate secondary antibody in blocking solution for 1 h at room temperature. Colocalization of FM1-43_{FX} (see above) and synapsin measures the fraction of presynaptic terminals that are functional.

Immunoprecipitation Assessment of A β Production. Neurons cultured conventionally (i.e., nonisland cultures) at high density were infected with appropriate virions for 1 h; then medium was replaced, and the cells were incubated for 2 h before replacement with methionine-free medium containing [³⁵S]methionine (0.5 mCi/ml) for 4 h. Medium and Triton X-100 cellular extracts were precleared with protein G-agarose, then they were immunopre-

cipitated with 6E10 (Signet Laboratories, Dedham, MA). Radiolabeled proteins were resolved on 4–16% Novex Bicine SDS/polyacrylamide gels, fixed, stained, dried, and exposed on phosphorimaging screens (Packard Instruments, Wellesley, MA) for 3–5 days. Band intensities were quantified by phosphorimager analysis.

Statistical Analysis. Data were analyzed with appropriate statistics, including unpaired Student's *t* test and ANOVA with a Dunnett's post hoc test. The multivariable comparison Dunnett's test allows for direct evaluation of any experimental group with

respect to the control population (i.e., uninfected and GFP-alone controls). All data are reported as mean \pm SEM.

We thank Hiro Watari for helpful discussion and Mike Ahlquist for fine work in cell culture. This work was supported by the University of Washington School of Medicine Alzheimer's Disease-Related Research Fund (to J.M.S.), an Alzheimer's Disease Research Center University of Washington Pilot Grant (to J.M.S.), the Klingenstein Fund (to J.M.S.), National Research Service Award Predoctoral Fellowship 1F31NS051906-01 from the National Institute of Neurological Disorders and Stroke (to J.T.T.), and T32 Postdoctoral Fellowship DA07278-10 from the National Institute on Drug Abuse (to B.G.K.).

1. LaFerla FM (2002) *Nat Rev Neurosci* 3:862–872.
2. Mattson MP (2004) *Nature* 430:631–639.
3. Selkoe DJ (2002) *Science* 298:789–791.
4. Small DH, Mok SS, Bornstein JC (2001) *Nat Rev Neurosci* 2:595–598.
5. Price DL, Sisodia SS (1998) *Annu Rev Neurosci* 21:479–505.
6. McGowan E, Eriksen J, Hutton M (2006) *Trends Genet* 22:281–289.
7. Wong PC, Cai H, Borchelt DR, Price DL (2002) *Nat Neurosci* 5:633–639.
8. Cleary JP, Walsh DM, Hofmeister JJ, Shankar GM, Kuskowski MA, Selkoe DJ, Ashe KH (2005) *Nat Neurosci* 8:79–84.
9. Janus C, Pearson J, McLaurin J, Mathews PM, Jiang Y, Schmidt SD, Chishti MA, Horne P, Heslin D, French J, et al. (2000) *Nature* 408:979–982.
10. Schenk D, Barbour R, Dunn W, Gordon G, Grajeda H, Guido T, Hu K, Huang J, Johnson-Wood K, Khan K, et al. (1999) *Nature* 400:173–177.
11. Billings LM, Oddo S, Green KN, McGaugh JL, LaFerla FM (2005) *Neuron* 45:675–688.
12. Dodart JC, Bales KR, Gannon KS, Greene SJ, DeMattos RB, Mathis C, DeLong CA, Wu S, Wu X, Holtzman DM, Paul SM (2002) *Nat Neurosci* 5:452–457.
13. Kotilinek LA, Bacskai B, Westerman M, Kawarabayashi T, Younkin L, Hyman BT, Younkin S, Ashe KH (2002) *J Neurosci* 22:6331–6335.
14. Kamenetz F, Tomita T, Hsieh H, Seabrook G, Borchelt D, Iwatsubo T, Sisodia S, Malinow R (2003) *Neuron* 37:925–937.
15. Almeida CG, Tampellini D, Takahashi RH, Greengard P, Lin MT, Snyder EM, Gouras GK (2005) *Neurobiol Dis* 20:187–198.
16. Roselli F, Tirard M, Lu J, Hutzler P, Lamberti P, Livrea P, Morabito M, Almeida OF (2005) *J Neurosci* 25:11061–11070.
17. Shemer I, Holmgren C, Min R, Fulop L, Zilberter M, Sousa KM, Farkas T, Hartig W, Penke B, Burnashev N, et al. (2006) *Eur J Neurosci* 23:2035–2047.
18. Snyder EM, Nong Y, Almeida CG, Paul S, Moran T, Choi EY, Nairn AC, Salter MW, Lombroso PJ, Gouras GK, Greengard P (2005) *Nat Neurosci* 8:1051–1058.
19. Chang EH, Savage MJ, Flood DG, Thomas JM, Levy RB, Mahadomrongkul V, Shirao T, Aoki C, Huerta PT (2006) *Proc Natl Acad Sci USA* 103:3410–3415.
20. Yao PJ, Zhu M, Pyun EI, Brooks AI, Therianos S, Meyers VE, Coleman PD (2003) *Neurobiol Dis* 12:97–109.
21. Citron M, Teplow DB, Selkoe DJ (1995) *Neuron* 14:661–670.
22. Zucker RS, Regehr WG (2002) *Annu Rev Physiol* 64:355–405.
23. Stevens CF, Williams JH (2000) *Proc Natl Acad Sci USA* 97:12828–12833.
24. Dobrunz LE, Stevens CF (1997) *Neuron* 18:995–1008.
25. Shrestha BR, Vitolo OV, Joshi P, Lordkipanidze T, Shelanski M, Dunaevsky A (2006) *Mol Cell Neurosci* 33:274–282.
26. Priller C, Bauer T, Mitteregger G, Krebs B, Kretschmar HA, Herms J (2006) *J Neurosci* 26:7212–7221.
27. Kelly BL, Vassar R, Ferreira A (2005) *J Biol Chem* 280:31746–31753.
28. Stevens CF, Sullivan JM (2003) *Neuron* 39:299–308.
29. Lundstrom K, Schweitzer C, Rotmann D, Hermann D, Schneider EM, Ehrengruber MU (2001) *FEBS Lett* 504:99–103.